

Which model density is best in pair natural orbital local correlation theory?

Réka A. Horváth, Kesha Sorathia, Isabelle Saint, and David P. Tew*

University of Oxford, South Parks Road, Oxford, OX1 3QZ, UK

(Dated: October 10, 2023)

Low-scaling electron correlation theory based on the pair natural orbital approximation, PNO-CCSD(T), has become a powerful computational tool. Motivated by the recent discovery of large errors for organometallic molecules, we assess the role of the model density used to discard unimportant contributions. We find that second-order perturbation theory provides the best compromise between cost and accuracy, but coupling between localised occupied orbitals must be accounted for. Errors in the CCSD energy are then well below 1 kcal/mol, even for molecules with moderate multi-reference character, and the primary remaining source of errors lies in the treatment of the (T) energy contribution.

I. INTRODUCTION

Low-scaling electron correlation theory has undergone considerable development over the past decade, and computational approaches have emerged^{1–4} capable of accurately computing heats of reaction and transition state energies of large molecular systems with modest computational resources.⁵ Although local approximations that exploit the short-ranged nature of electron correlation in molecules were introduced many years ago,^{6–9} in practice, the sizable errors resulting from the domain approximation¹⁰ prevented widescale application. In 2009 Neese re-introduced¹¹ pair natural orbital (PNO) theory,¹² which made it possible to use large local domains and eliminate instabilities arising from the domain approximation. The PNO-CCSD(T) method (coupled cluster with singles, doubles and perturbative triples), has emerged as practical alternative to density functional theory for computational studies, particularly in organometallic chemistry, which requires accurate description of exchange, delocalisation and dispersion interactions.

In PNO coupled-cluster theory, each pair-correlation function $|\mu_{ij}\rangle$ is expanded using a pair-specific subset of virtuals, whose number v_{ij} and character are determined to recover the correlation energy for that orbital pair to a target accuracy

$$|\mu_{ij}\rangle = \frac{1}{2} \sum_{\bar{a}\bar{b}}^{v_{ij}} t_{\bar{a}\bar{b}}^{ij} \hat{E}_{i\bar{a}} \hat{E}_{j\bar{b}} |0\rangle. \quad (1)$$

Here the excitation operator $\hat{E}_{i\bar{a}} = \hat{a}_{\bar{a}\alpha}^\dagger \hat{a}_{i\alpha} + \hat{a}_{\bar{a}\beta}^\dagger \hat{a}_{i\beta}$ promotes an electron from a localised occupied orbital i to pair natural virtual orbital \bar{a} . $|0\rangle$ is the Hartree-Fock reference wavefunction. Pair natural orbitals diagonalise the pair correlation density

$$D_{ab} = 2 \sum_c [\bar{t}_{ac}^{ij} t_{bc}^{ij} + \bar{t}_{ca}^{ij} t_{cb}^{ij}] \quad (2)$$

$$\sum_{ab} U_{a\bar{a}}^\dagger D_{ab} U_{b\bar{b}} = N_{\bar{a}} \delta_{\bar{a}\bar{b}} \quad (3)$$

and provide a maximally convergent expansion for the correlation function.¹³ Here $\bar{t}_{ac}^{ij} = 2t_{ac}^{ij} - t_{ca}^{ij}$. The size of

the PNO space v_{ij} for each pair is set by retaining PNOs with $N_{\bar{a}} \geq \mathcal{T}$, where the PNO threshold \mathcal{T} determines the accuracy of the resulting correlation energy. Formally, t_{ab}^{ij} is the amplitude for the pair excitation in canonical coupled-cluster theory. In practice, approximate amplitudes \tilde{t}_{ab}^{ij} are used to construct a model density to determine the PNOs.¹⁴ The ensuing coupled-cluster calculation is performed at low cost in the retained subset of PNOs and the contribution to the model amplitudes from the discarded PNOs is added as an energy correction term.¹¹ The PNO approach is predicated on the assumption that the orbitals obtained from the approximate amplitudes are also appropriate for representing the coupled cluster wavefunction. This letter addresses that assumption and asks the title question: which model density is best in pair natural orbital local correlation theory?

The standard approach is to use first-order amplitudes from Møller-Plesset perturbation theory to form the model density. Often a semi-canonical approximation is used that neglects off-diagonal Fock matrix elements f_i^j among the localised occupied orbitals.

$$\tilde{t}_{ab}^{ij} = -\frac{g_{ab}^{ij}}{\epsilon_a + \epsilon_b - f_i^i - f_j^j} \quad (4)$$

where $g_{ab}^{ij} = \langle ia|jb\rangle$ are the electron repulsion integrals and ϵ_a the canonical orbital eigenvalues. Generally, the energy from a PNO-CCSD(T) calculation $E(\mathcal{T})$ converges to the canonical result E as the threshold \mathcal{T} is reduced, and the size of the PNO space increases, according to the power law^{15,16}

$$E(\mathcal{T}) = E + A\mathcal{T}^{1/2} \quad (5)$$

To obtain accurate energies for the reliable prediction of chemical phenomena, it is necessary to ensure that the PNO truncation error $A\mathcal{T}^{1/2}$ is under control. Neese and co-workers demonstrated¹⁷ that mean absolute PNO truncation errors with $\mathcal{T} = 10^{-7}$ are around 0.5 kcal/mol or less in PNO-CCSD(T) calculations for the GMTKN55 data set,¹⁸ which includes reaction energies and isomerisation energies of small and large molecules, intermolecular and intramolecular non-covalent interaction energies and reaction barrier heights.

However, for systems with a higher proportion of static correlation, PNO truncation errors can be several kcal/mol, and $\mathcal{T} = 10^{-8}$ or PNO extrapolation is necessary.^{16,19} This is evident from the work of Martin and co-workers²⁰ on metal organic barrier heights²¹ and expanded porphyrin macrocycles that can interconvert between Hückel, figure-of-eight, and Möbius topologies.²²

The large PNO truncation errors are an indication that the MP2 pair correlation density may fail to accurately model the CCSD pair correlation density for these systems, reducing the proportion of correlation energy recovered in the selected PNO subspace and reducing the accuracy of the energy estimate for the discarded PNOs.

We have therefore implemented the possibility, within the `pnoccsd` module in the Turbomole program package,²³ to perform a hierarchy of intermediate methods between MP2 theory and CCSD theory, to obtain the corresponding model density, and to perform PNO-CCSD(T) calculations using PNOs obtained from any of these model densities. The accuracy of each model can be assessed through the size of the PNO truncation error for computed PNO-CCSD(T) correlation energies.

If accuracy were the only criteria, then the answer to the title question would be trivial. The most accurate model density is obviously that obtained from the canonical CCSD amplitudes, but this is of no practical use when designing low-cost correlation methods. “Best” here refers to the best compromise between accuracy and the cost incurred to obtain the model density.

The doubles amplitude equations for our chosen models are

$$0 = \langle \bar{a}b | \tilde{H} + [\tilde{H}, \hat{T}_2] + \frac{1}{2} [[\tilde{H}, \hat{T}_2], \hat{T}_2] | 0 \rangle \quad \text{CCSD} \quad (6)$$

$$0 = \langle \bar{a}b | \hat{H} + [\hat{H}, \hat{T}_2] + \frac{1}{2} [[\hat{H}, \hat{T}_2], \hat{T}_2] | 0 \rangle \quad \text{CCD} \quad (7)$$

$$0 = \langle \bar{a}b | \tilde{H} + [\tilde{H}, \hat{T}_2] | 0 \rangle \quad \text{LCCSD} \quad (8)$$

$$0 = \langle \bar{a}b | \hat{H} + [\hat{H}, \hat{T}_2] | 0 \rangle \quad \text{LCCD} \quad (9)$$

$$0 = \langle \bar{a}b | \tilde{H} + [\tilde{H}, \hat{T}_2] | 0 \rangle \quad \text{CC2} \quad (10)$$

$$0 = \langle \bar{a}b | \hat{H} + [\hat{H}, \hat{T}_2] | 0 \rangle \quad \text{MP2} \quad (11)$$

where \tilde{H} is the T_1 transformed Hamiltonian $e^{-\hat{T}_1} \hat{H} e^{\hat{T}_1}$ and $\langle \bar{a}b |$ are the biorthogonal bra states for the doubles projection manifold. The methods CCD and LCCD are obtained from CCSD and LCCSD, respectively, by setting all T_1 amplitudes to zero so that $\tilde{H} = \hat{H}$. The singles amplitude equations for CC2 and LCCSD are the same as for CCSD

$$0 = \langle a | \tilde{H} + [\tilde{H}, \hat{T}_2] | 0 \rangle \quad (12)$$

To assess the accuracy of each model, we chose to perform calculations on the MOBH35 data set of barrier heights for organometallic reactions²¹ and the POLYPYR21 data set of Hückel-Möbius porphyrin macrocycles,²² which contain species with moderate amounts of static correlation and large PNO truncation errors. Although triple-zeta quality basis sets are the minimum required to obtain

reliable CCSD(T) energies for comparison with experiment, the behaviour of the PNO truncation error is very similar across basis sets.^{16,17} We therefore use double-zeta quality basis sets in this work.

Two measures of accuracy are used to assess each model density. The first, Q_d , is a direct measure of the proportion of the CCSD density discarded when truncating the space using PNOs from a model density; the second, Q_e , is the error in the correlation energy incurred when the selected model PNOs are used in a PNO-CCSD(T) calculation.

We define $Q_d(\mathcal{T})$ as the average density lost per pair using PNO truncation threshold \mathcal{T}

$$Q_d(\mathcal{T}) = \frac{1}{n_{ij}} \sum_{i \leq j} (\text{Tr}[\mathbf{D}^{ij}] - \text{Tr}[\tilde{\mathbf{D}}^{ij}(\mathcal{T})]) / \text{Tr}[\mathbf{D}^{ij}] \quad (13)$$

$$\tilde{D}_{\bar{a}\bar{b}}^{ij} = \sum_{ab} U_{a\bar{a}}^{ij} D_{ab}^{ij} U_{b\bar{b}}^{ij} \quad (14)$$

Here the CCSD pair correlation density \mathbf{D}^{ij} formally has the $v \times v$ dimension of the full virtual space, $\tilde{\mathbf{D}}^{ij}(\mathcal{T})$ is the truncated pair density that has the $v_{ij} \times v_{ij}$ dimension of the retained PNOs at threshold \mathcal{T} , and $U_{a\bar{a}}^{ij}$ is the transformation matrix from v canonical virtuals to the v_{ij} PNOs for pair ij obtained from the chosen model density at threshold \mathcal{T} . By plotting $Q_d(\mathcal{T})$ against the average dimension $v_{ij}(\mathcal{T})$ as a function of \mathcal{T} for each model density, we can compare the relative accuracy of each model.

We define $Q_e(\mathcal{T})$ as the error in the CCSD(T) correlation energy using the PNOs from the model density and truncation threshold \mathcal{T} . It is composed of three terms

$$Q_e(\mathcal{T}) = \mathcal{E}_{\text{SD}}(\mathcal{T}) + \mathcal{E}_{\text{T}}(\mathcal{T}) - \Delta(\mathcal{T}) \quad (15)$$

\mathcal{E}_{SD} is the error in the CCSD correlation energy and \mathcal{E}_{T} is the error in the (T) energy. The \mathcal{E}_{T} contribution depends primarily on the truncation of the triples space through the selection of triple natural orbitals,²⁴ which is independent of the chosen pair density model in the current implementation.²⁵ Variations in \mathcal{E}_{T} among model densities are a reflection of the accuracy of the T_2 amplitudes used to compute the (T) energy.

The Δ term corrects for \mathcal{E}_{SD} and is the energy estimate for the discarded PNOs based on the model amplitudes

$$\Delta = \sum_{ij} \left(\sum_{ab} \tilde{t}_{ab}^{ij} \bar{g}_{ij}^{ab} - \sum_{\bar{a}\bar{b}} \tilde{t}_{\bar{a}\bar{b}}^{ij} \bar{g}_{ij}^{\bar{a}\bar{b}} \right) \quad (16)$$

Here $\bar{g}_{ij}^{ab} = 2g_{ij}^{ab} - g_{ij}^{ba}$. We report error statistics in units of mE_h per valence electron for total energies, and in kcal/mol for reaction energies and barrier heights.

II. COMPUTATIONAL DETAILS

The structures for the MOBH35 test set were taken from the supporting information of Ref 20, where the

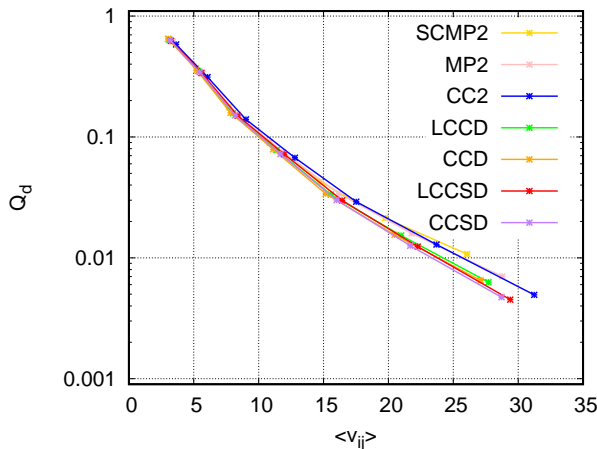


FIG. 1: The loss of information against average number of PNOs for different model densities for reactant 29 of the MOBH35 set

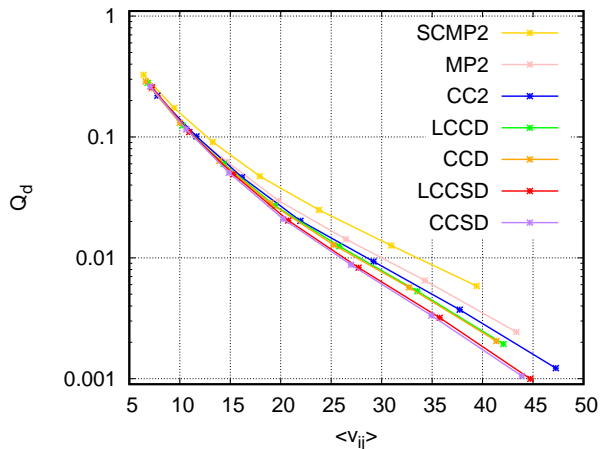


FIG. 2: The loss of information against average number of PNOs for different model densities for reactant 32 of the MOBH35 set

transition state structures for reactions 11 and 12, and all species of reaction 14 are modified from the original data set, as recommended by Dohm *et al.*²⁶ We use the def2-SVP²⁷ basis and density fitting basis²⁸ and the Stuttgart relativistic effective core potentials²⁹ for molecules containing second- and third-row transition metal atoms. Reactant 16 converges to the incorrect state if the default extended Hückel orbital guess is applied and an orbital swap was required to obtain the correct initial electronic configuration. Canonical CCSD(T) energies for 19 of the 35 reactions are available from earlier work,¹⁶ so we use this subset MOBH19 for the current study. These are reactions 3, 4, 6, 7, 13, 14, 15, 16, 21, 23, 26, 27, 29, 30, 31, 32, 33, 34 and 35.

The structures for the POLYPYR21 data set were taken from the supporting information of Ref. 22. To enable direct comparison with the CCSD and CCSD(T) energies of the original work, we use the cc-pVDZ basis set³⁰ with the *d* functions on the H atoms removed, and the cc-pVDZ density fitting basis.³¹

All calculations were performed using the the `dscf`³² and `pnocsd` modules,^{2,25,33} of the Turbomole package. Density fitting was not used in the Hartree-Fock calculations. Orbitals were localised using the intrinsic bond orbital method.³⁴ and in all cases the multi-level approximation^{35,36} were not applied. The Q_d and Q_e measures were computed from near-canonical model densities obtained from the corresponding PNO coupled cluster calculation using a very tight PNO threshold of $\mathcal{T}=10^{-9}$. Where timings are reported, these were performed on a single Intel(R) Xeon(R) Gold 6248R CPU @ 3.00GHz node with 48 cores, 380 Gb RAM and 1.8Tb SSD.

III. RESULTS

Figs. 1 and 2 display the average information lost $Q_d(\mathcal{T})$ against the average number of PNOs $v_{ij}(\mathcal{T})$ retained with $\mathcal{T}=10^{-5}$ – 10^{-8} for the hierarchy of model densities. The two chosen molecules r29 and r32 are the extremal cases of the MOBH19 set where the SCMP2 density performs best and worst relative to CCSD, respectively. The CCSD model loses the least possible information per PNO discarded and is the reference against which the other methods are judged.

The LCCSD and LCCD models are only marginally inferior to CCSD and CCD, respectively. The influence of the quadratic T_2 terms in the CC model are therefore small on average. We find that they are more significant for strong pairs than weak pairs, but in most cases have less impact than the singles cluster amplitudes. Particularly for molecules with substantial correlation-induced orbital relaxation, the CCD and LCCD models lose accuracy relative to CCSD and CC2 is more accurate than MP2. In almost all cases MP2 is significantly better than semi-canonical MP2. Neglecting the Fock matrix elements that couple the localised orbitals is a poor approximation. Overall, the accuracy of the CC model densities is in line with that expected from a perturbative analysis of the the amplitude equations, and the magnitude of the interaction follows $f_i^j > [\hat{H}, T_2] > T_1 > [[\hat{H}, T_2], T_2]$.

Fig. 3 shows the mean absolute truncation error per valence electron in the CCSD correlation energy against the mean number of PNOs per pair, averaged over the dat set, for $\mathcal{T}=10^{-5}$ – 10^{-8} . For each model density, we plot the mean absolute values of \mathcal{E}_{SD} and $\mathcal{E}_{SD} - \Delta$, to ascertain the relative accuracy of the energy estimate for the discarded PNOs. The mean \mathcal{E}_{SD} values for each method mirror the trend observed for Q_d , with

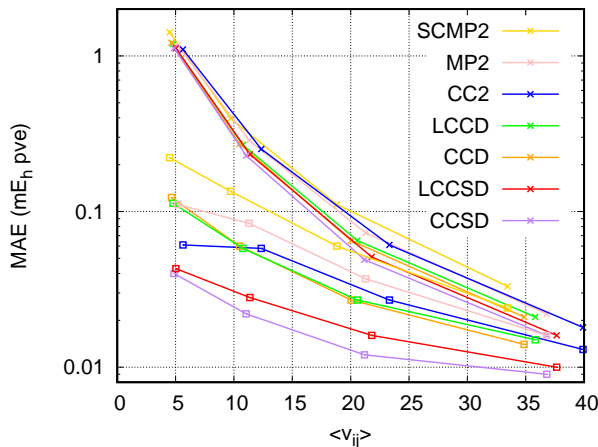


FIG. 3: Mean absolute PNO truncation errors \mathcal{E}_{SD} (\times) and $\mathcal{E}_{\text{SD}} - \Delta$ (\square) against the average number of PNOs for the MOBH19 set using various model densities

$\text{CCSD} \sim \text{LCCSD} < \text{CCD} \sim \text{LCCD} < \text{CC2} \sim \text{MP2} < \text{SCMP2}$.

A greater variation in accuracy is observed for $\mathcal{E}_{\text{SD}} - \Delta$, but again the same trend is observed. However, we find that the CC2 model is significantly more accurate than MP2 when the Δ correction is taken into account. Interestingly, for CCSD, the Δ correction does not entirely eliminate the PNO truncation error, and a small error remains due to relaxation of the T_2 amplitudes when solving the non-linear CCSD equations in the retained subspace.

In Table I we report statistical measures for the distribution of PNO truncation errors in the barrier heights of the MOBH19 set. From the data for the CCSD model,

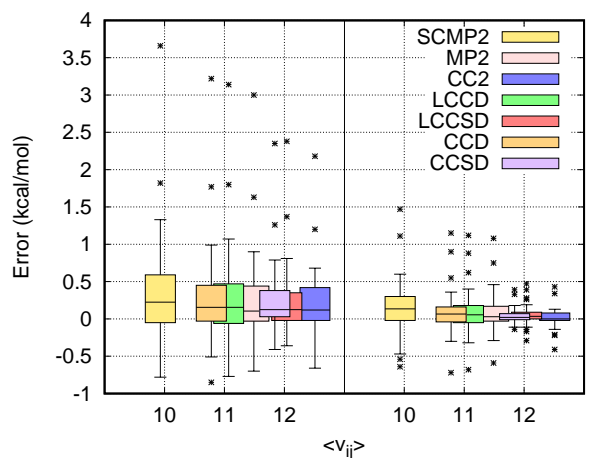


FIG. 4: Box plots for PNO-CCSD errors \mathcal{E}_{SD} (left) and $\mathcal{E}_{\text{SD}} - \Delta$ (right) in MOBH19 barrier heights using $\mathcal{T}=10^{-6}$.

we see that for both \mathcal{E}_{SD} and $\mathcal{E}_{(\text{T})}$ the 2σ 95% confidence interval falls within 1 kcal/mol only for $\mathcal{T}=10^{-7}$ and tighter. The \mathcal{E}_{SD} contribution is almost entirely removed by the Δ correction and the error in the (T) energy becomes the limiting factor. All of the approximate models follow this same pattern.

Fig. 4 displays box plots for the PNO truncation errors in the PNO-CCSD barrier heights of the MOBH19 set, with and without the correction for discarded PNOs, using the various model densities with $\mathcal{T}=10^{-6}$. Fig. 5 displays the corresponding information for $\mathcal{T}=10^{-7}$. To indicate the accuracy relative to the subspace size, the data for each method is positioned along the x axis at the average of $\langle v_{ij} \rangle$ for the transition states.

From the table and the figures, we see that for a given threshold \mathcal{T} , the CC2 model gives the smallest errors, but this is because it predicts a larger density and therefore more PNOs are retained. Nevertheless, the Δ correction with the CC2 model appears to be particularly accurate. The ratio of accuracy to number of PNOs for barrier heights using the model densities follows the same trend as that seen for total energies and information content. The MP2 model is remarkably accurate overall and the benefit of using higher-order CC models appears marginal, especially since the (T) error is the dominant contribution.

The $\mathcal{E}_{(\text{T})}$ statistics are very similar for all methods. The primary factor in $\mathcal{E}_{(\text{T})}$ is the model density used for the TNO truncation, which is independent of the PNO model density in this work. The error in the (T) energy due to errors in the T_2 amplitudes are smaller, but not insignificant, and give rise to some variation among the model densities tested. We find that the maximum errors are generally smaller for CC2 and LCCSD than for LCCD and CCD. Overall, the SCMP2 performs the worst, and

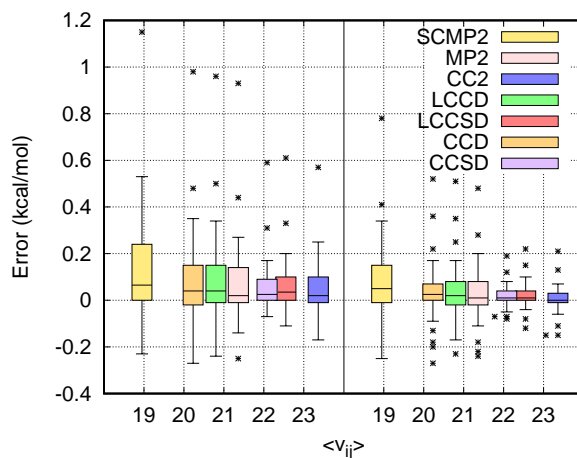


FIG. 5: Box plots for PNO-CCSD errors \mathcal{E}_{SD} (left) and $\mathcal{E}_{\text{SD}} - \Delta$ (right) in MOBH19 barrier heights using $\mathcal{T}=10^{-7}$.

TABLE I: PNO truncation error normal distributions (μ, σ_n) for barrier heights of the MOBH19 set in kcal/mol

Contr.	\mathcal{T}	SCMP2		MP2		CC2		LCCD		CCD		LCCSD		CCSD	
		μ	σ	μ	σ	μ	σ	μ	σ	μ	σ	μ	σ	μ	σ
\mathcal{E}_{SD}	10^{-5}	1.23	2.06	0.94	1.72	0.78	1.50	1.12	1.99	1.13	2.03	0.98	1.79	1.03	1.78
	10^{-6}	0.37	0.74	0.27	0.61	0.20	0.46	0.30	0.64	0.29	0.65	0.24	0.50	0.23	0.48
	10^{-7}	0.12	0.24	0.08	0.19	0.04	0.12	0.09	0.20	0.09	0.20	0.06	0.12	0.06	0.12
	10^{-8}	0.03	0.09	0.02	0.07	0.01	0.05	0.03	0.07	0.02	0.07	0.02	0.05	0.01	0.04
$\mathcal{E}_{\text{SD}} - \Delta$	10^{-5}	0.20	0.73	0.08	0.48	-0.03	0.34	0.16	0.55	0.16	0.55	0.09	0.28	0.04	0.19
	10^{-6}	0.15	0.38	0.08	0.27	0.02	0.14	0.10	0.30	0.09	0.30	0.05	0.14	0.04	0.10
	10^{-7}	0.08	0.18	0.03	0.12	0.01	0.06	0.04	0.13	0.04	0.13	0.02	0.06	0.01	0.05
	10^{-8}	0.02	0.08	0.01	0.06	0.01	0.04	0.02	0.06	0.01	0.07	0.01	0.04	0.01	0.04
$\mathcal{E}_{(\text{T})}$	10^{-5}	0.78	1.41	0.62	1.09	0.61	1.05	0.62	1.14	0.64	1.17	0.64	1.09	0.64	1.09
	10^{-6}	0.41	0.73	0.28	0.55	0.28	0.51	0.29	0.58	0.30	0.59	0.29	0.53	0.29	0.54
	10^{-7}	0.16	0.31	0.11	0.24	0.11	0.22	0.12	0.25	0.12	0.26	0.11	0.22	0.11	0.22
	10^{-8}	0.05	0.11	0.04	0.09	0.03	0.08	0.04	0.09	0.04	0.10	0.04	0.08	0.04	0.09
Q_e	10^{-5}	0.98	1.84	0.70	1.34	0.58	1.06	0.78	1.52	0.80	1.56	0.72	1.21	0.68	1.14
	10^{-6}	0.56	1.06	0.36	0.77	0.30	0.59	0.38	0.82	0.39	0.84	0.34	0.63	0.33	0.60
	10^{-7}	0.24	0.47	0.14	0.34	0.12	0.26	0.16	0.36	0.16	0.37	0.13	0.26	0.13	0.26
	10^{-8}	0.08	0.19	0.05	0.14	0.04	0.11	0.05	0.15	0.05	0.15	0.04	0.11	0.05	0.11

the majority of the available improvement is obtained already at the MP2 level. Using MP2 or CC2 model densities with $\mathcal{T}=10^{-7}$ is sufficient to reduce the maximum total PNO truncation errors to within 1 kcal/mol.

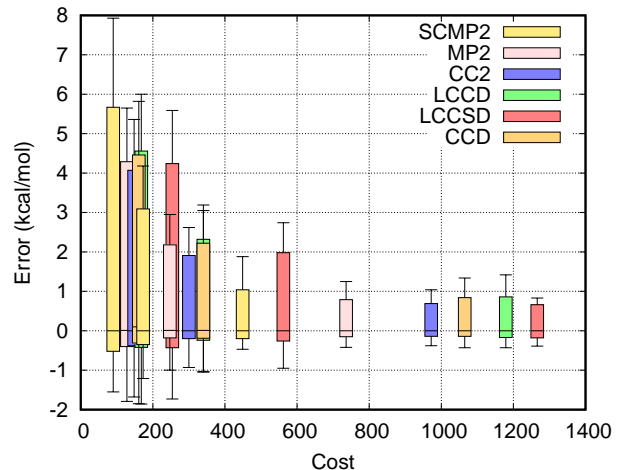
The cost of using a higher-order CC model to obtain an approximate density has two sources: the overhead of performing the higher-order CC model using a tight threshold; and a cost or benefit arising from a larger or smaller PNO set for the subsequent PNO-CCSD(T) calculation. The overhead can be reduced by loosening the PNO threshold used to obtain the model density.

In Table II we list the mean absolute and maximum errors using the MP2 and CC2 model densities computed using a threshold of $0.1\mathcal{T}$, compared to the near-canonical densities obtained with 10^{-9} . The errors obtained using the SCMP2 density are included for comparison. Evidently, using a threshold of $0.1\mathcal{T}$ is sufficient to recover more than two-thirds of the available improvement over SCMP2 on average, but the outliers are significantly improved if the Δ correction spans the larger PNO space.

In Fig. 6 we report the error statistics for the POLYPYR21 set using $\mathcal{T}=10^{-6}$, 10^{-7} and 10^{-8} and a threshold of $0.1\mathcal{T}$ for the model density. To provide a direct measure of the cost, we compute a weighted sum

TABLE II: Mean absolute (and maximum) PNO-CCSD errors for MOBH19 barriers in kcal/mol

Density	$\mathcal{T} = 10^{-5}$	$\mathcal{T} = 10^{-6}$	$\mathcal{T} = 10^{-7}$
SCMP2 (10^{-9})	0.51 (2.61)	0.28 (1.47)	0.13 (0.78)
MP2 (0.1 \mathcal{T})	0.38 (1.45)	0.22 (1.20)	0.09 (0.54)
MP2 (10^{-9})	0.31 (1.80)	0.18 (1.08)	0.08 (0.48)
CC2 (0.1 \mathcal{T})	0.26 (0.78)	0.14 (0.80)	0.06 (0.34)
CC2 (10^{-9})	0.23 (1.11)	0.08 (0.43)	0.04 (0.21)

FIG. 6: Box plots for PNO-CCSD(T) errors of the POLYPYR21 set using different model densities with $\mathcal{T}=10^{-6}$, 10^{-7} and 10^{-8} .

of the wall times in seconds for the test set, where the weight for each molecule is the reciprocal of the size of the AO basis. The box plot for each model and threshold is positioned along the x axis at the value of the corresponding cost measure.

The PNO truncation errors for $\mathcal{T}=10^{-6}$ are up to 8 kcal/mol. The PNO approximation with this threshold introduces an error so large that almost no benefit from the sophisticated coupled-cluster wavefunction model remains. Even with $\mathcal{T}=10^{-7}$, errors are as much as 4 kcal/mol for the Möbius structures. With the SCMP2 model density and $\mathcal{T}=10^{-8}$, some PNO errors of 2 kcal/mol remain. However, if the MP2, CC2 or LCCSD

TABLE III: PNO truncation errors for CCSD energies of the POLYPYR21 set in kcal/mol

System	Molpro	Orca	MRCC	SCMP2 ^a	MP2 ^{a,b}
24H _a	0.1	0.0	0.0	0.0	0.0
24H _b	0.0	0.0	0.0	0.0	0.0
24M	0.3	0.1	0.1	0.1	0.1
24TS ₁	-0.1	0.0	0.1	0.0	0.0
24TS ₂	0.1	0.0	0.1	0.1	0.0
28F	-0.2	-0.6	-0.5	-0.2	0.0
28M _{1A}	2.0	0.5	0.3	0.3	0.3
28M	1.8	0.7	0.2	0.4	0.4
28M _{1B}	2.2	0.5	0.2	0.4	0.4
28TS ₃	0.0	-0.1	-0.4	0.0	0.0
28H	0.0	0.0	0.0	0.0	0.0
28TS _{1A}	0.2	0.3	0.3	0.2	0.1
28TS _{1B}	-0.1	-0.1	-0.4	0.0	0.0
28TS _{2A}	2.4	1.0	0.2	0.6	0.4
28TS _{2B}	2.0	0.8	0.2	0.6	0.5
32F	0.0	0.0	0.0	0.0	0.0
32H	-0.7	0.5	0.4	0.3	-0.1
32TS ₂	-0.7	0.5	0.3	0.2	-0.1
32M _a	1.4	0.8	1.2	0.8	0.4
32M _b	2.2	1.2	1.0	0.9	0.6
32TS ₁	-0.3	0.1	0.1	0.1	0.0
RMS	1.3	0.6	0.5	0.4	0.3

^a Turbomole ^b This work

model densities are used, errors approach the reliability target of 1 kcal/mol. Among these, the MP2 model is the cheapest.

The timings used for the figure are only indicative, since the implementation of each approach has not been fully optimised. Nevertheless, we note some interesting trends in the relative costs of using the model densities. For example, LCCD is more expensive than CCD. This is because, although each iteration is cheaper, the LCCD equations take longer to converge. The CC2 model is much more expensive than MP2, both because the number of retained PNOs is higher, and because the singles residual contains long-ranged Fock-like terms that are expensive to evaluate. The cost of the MP2 model can probably be reduced to close to that of the SCMP2 model by use of the Laplace transform approach.³⁷

In Table III we report the PNO truncation errors using the SCMP2 and MP2 model densities for PNO-CCSD energies of the POLYPYR21 set, compared to those reported in Ref. 22 using the PNO-CCSD implementations in ORCA³⁸ and Molpro³⁹, and using the LNO-CCSD implementation in MRCC.⁴⁰ In all cases, a threshold corresponding to $\mathcal{T}=10^{-7}$ is used. The differences among the Molpro, Orca and Turbomole PNO implementations are most likely due to the differing domain sizes and multi-level pair approximations. Using the full MP2 density instead of the semi-canonical density to determine the PNOs ensures that the root mean squared (RMS) CCSD error is 0.3 kcal/mol with a maximum error of only 0.6 kcal/mol for the challenging Möbius structures.

The truncation error in the PNO-CCSD(T) energies,

in Fig. 6 is dominated by the (T) energy contribution. The RMS error rises from 0.3 kcal/mol for CCSD to 1.6 kcal/mol for CCSD(T), when using the MP2 model density for the PNO space. The maximum error rises from 0.6 to 3.0 kcal/mol. The truncation error can be reduced through two-point extrapolation assuming Eq. 5. Application of two-point extrapolation of PNO-CCSD(T) energies using $\mathcal{T}=10^{-6}$ and $\mathcal{T}=10^{-7}$ data reduces RMS and maximum errors to 0.9 kcal/mol and 1.7 kcal/mol, respectively. Nevertheless, the primary remaining bottleneck in accuracy for PNO calculations on systems with moderate static correlation is treatment of the (T) energy contribution.

IV. CONCLUSIONS

We set out to investigate the extent to which the model density used to construct the PNOs impacts the PNO truncation errors in local correlation theory and to answer the title question "which model density is best?" by assessing the relative cost-benefit ratios of a hierarchy of model densities, starting with semi-canonical MP2 theory and ending with full CCSD. We were motivated to address this question by the observation that large truncation errors are observed for transition metal containing systems with moderate static correlation, where canonical coupled-cluster theory is expected to provide accurate predictions.⁴¹⁻⁴³

We find that even when using the best possible model density, CCSD itself, the energy converges slowly with PNO truncation threshold for systems with a high degree of multi-reference character. Provided that the Fock terms f_i^j are not neglected in the model, there is only a modest improvement of the PNO space when using CCSD instead of MP2 for these systems. However, the quality of the model density does greatly impact the accuracy of the energy correction for discarded PNOs. We find that coupling to the singles amplitudes is more important than higher-order doubles terms in the CC model.

In the context of practical low-scaling electronic structure approaches, the two candidates for best cost-to-accuracy ratios are therefore the MP2 and CC2 models. Due to the significant additional cost of computing the singles residual for CC2, our recommendation is to use the MP2 model. The application of the semi-canonical approximation leads to a substantial deterioration of both the PNOs and the energy correction term and should be avoided.

Using the MP2 density, errors in the CCSD energy are well below 1 kcal/mol with $\mathcal{T}=10^{-7}$ and the primary remaining error arises from the truncation of the triples space when computing the (T) energy. Although not tested in this work, these conclusions are equally applicable to the explicitly-correlated variants of local correlation theory.^{2,44-47}

- * david.tew@chem.ox.ac.uk
- ¹ Christoph Riplinger, Peter Pinski, Ute Becker, Edward F. Valeev, and Frank Neese, "Sparse maps—A systematic infrastructure for reduced-scaling electronic structure methods. II. Linear scaling domain based pair natural orbital coupled cluster theory," *J. Chem. Phys.* **144**, 024109 (2016).
 - ² Gunnar Schmitz, Christof Hättig, and David P. Tew, "Explicitly correlated pno-mp2 and pno-ccsd and their application to the s66 set and large molecular systems," *Phys. Chem. Chem. Phys.* **16**, 22167–22178 (2014).
 - ³ Qianli Ma and Hans-Joachim Werner, "Explicitly correlated local coupled-cluster methods using pair natural orbitals," *WIREs Comput. Mol. Sci.* **8**, e1371 (2018).
 - ⁴ Péter R. Nagy and Mihály Kállay, "Approaching the basis set limit of ccsd(t) energies for large molecules with local natural orbital coupled-cluster methods," *J. Chem. Theory Comput.* **15**, 5275–5298 (2019).
 - ⁵ Yannick J. Franzke, Christof Holzer, Josefine H. Andersen, Tomislav Begušić, Florian Bruder, Sonia Coriani, Fabio Della Sala, Eduardo Fabiano, Daniil A. Fedotov, Susanne First, Sebastian Gillhuber, Robin Grotjahn, Martin Kaupp, Max Kehry, Marjan Krstić, Fabian Mack, Sourav Majumdar, Brian D. Nguyen, Shane M. Parker, Fabian Pauly, Ansgar Pausch, Eva Perlt, Gabriel S. Phun, Ahmadreza Rajabi, Dmitriy Rapoport, Bibek Samal, Tim Schrader, Manas Sharma, Enrico Tapavicza, Robert S. Treß, Vamsee Voora, Artur Wodyński, Jason M. Yu, Benedikt Zerulla, Philipp Furche, Christof Hättig, Marek Sierka, David P. Tew, and Florian Weigend, "Turbomole: Today and tomorrow," *J. Chem. Theory Comput.* **0**, null (0).
 - ⁶ Oktay Sinanoğlu, "Many-electron theory of atoms, molecules and their interactions," in *Adv. Chem. Phys.* (John Wiley & Sons, Ltd, 1964) pp. 315–412.
 - ⁷ Peter Pulay, "Localizability of dynamic electron correlation," *Chem. Phys. Lett.* **100**, 151–154 (1983).
 - ⁸ Svein Sæbø and Peter Pulay, "Local configuration interaction: An efficient approach for larger molecules," *Chem. Phys. Lett.* **113**, 13–18 (1985).
 - ⁹ Martin Schütz, Georg Hetzer, and Hans Joachim Werner, "Low-order scaling local electron correlation methods. I. Linear scaling local MP2," *J. Chem. Phys.* **111**, 5691–5705 (1999).
 - ¹⁰ James W. Boughton and Peter Pulay, "Comparison of the boys and pipek-mezey localizations in the local correlation approach and automatic virtual basis selection," *J. Comput. Chem.* **14**, 736–740 (1993).
 - ¹¹ Frank Neese, Frank Wennmohs, and Andreas Hansen, "Efficient and accurate local approximations to coupled-electron pair approaches: An attempt to revive the pair natural orbital method," *J. Chem. Phys.* **130**, 114108 (2009).
 - ¹² Per-Olov Löwdin, "Quantum theory of many-particle systems. i. physical interpretations by means of density matrices, natural spin-orbitals, and convergence problems in the method of configurational interaction," *Phys. Rev.* **97**, 1474–1489 (1955).
 - ¹³ Per-Olov Löwdin and Harrison Shull, "Natural orbitals in the quantum theory of two-electron systems," *Phys. Rev.* **101**, 1730–1739 (1956).
 - ¹⁴ Wilfried Meyer, "PNO–CI Studies of electron correlation effects. I. Configuration expansion by means of nonorthogonal orbitals, and application to the ground state and ionized states of methane," *J. Chem. Phys.* **58**, 1017–1035 (1973).
 - ¹⁵ Kesha Sorathia and David P. Tew, "Basis set extrapolation in pair natural orbital theories," *J. Chem. Phys.* **153**, 174112 (2020).
 - ¹⁶ Kesha Sorathia, Damyan Frantsov, and David P. Tew, "Improved cps and cbs extrapolation of pno-ccsd(t) energies: The mobh35 and isol24 data sets," (2023), arXiv:2309.02639 [physics.chem-ph].
 - ¹⁷ Dimitrios G. Liakos, Yang Guo, and Frank Neese, "Comprehensive benchmark results for the domain based local pair natural orbital coupled cluster method (dlpno-ccsd(t)) for closed- and open-shell systems," *J. Phys. Chem. A* **124**, 90–100 (2020).
 - ¹⁸ Lars Goerigk, Andreas Hansen, Christoph Bauer, Stephan Ehrlich, Asim Najibi, and Stefan Grimme, "A look at the density functional theory zoo with the advanced gmtkn55 database for general main group thermochemistry, kinetics and noncovalent interactions," *Phys. Chem. Chem. Phys.* **19**, 32184–32215 (2017).
 - ¹⁹ Ahmet Altun, Frank Neese, and Giovanni Bistoni, "Extrapolation to the limit of a complete pair natural orbital space in local coupled-cluster calculations," *J. Chem. Theory Comput.* **16**, 6142–6149 (2020).
 - ²⁰ Emmanouil Semidalas and Jan M.L. Martin, "The mobh35 metal–organic barrier heights reconsidered: Performance of local-orbital coupled cluster approaches in different static correlation regimes," *J. Chem. Theory Comput.* **18**, 883–898 (2022).
 - ²¹ Mark A. Iron and Trevor Janes, "Evaluating transition metal barrier heights with the latest density functional theory exchange–correlation functionals: The mobh35 benchmark database," *J. Phys. Chem. A* **123**, 3761–3781 (2019).
 - ²² Nitai Sylvetsky, Ambar Banerjee, Mercedes Alonso, and Jan M. L. Martin, "Performance of localized coupled cluster methods in a moderately strong correlation regime: Hückel–möbius interconversions in expanded porphyrins," *J. Chem. Theory Comput.* **16**, 3641–3653 (2020).
 - ²³ "TURBOMOLE V7.7 2023, a development of University of Karlsruhe and Forschungszentrum Karlsruhe GmbH, 1989–2007, TURBOMOLE GmbH, since 2007; available from <http://www.turbomole.com>,".
 - ²⁴ Christoph Riplinger, Barbara Sandhoefer, Andreas Hansen, and Frank Neese, "Natural triple excitations in local coupled cluster calculations with pair natural orbitals," *J. Chem. Phys.* **139**, 134101 (2013).
 - ²⁵ Gunnar Schmitz and Christof Hättig, "Perturbative triples correction for local pair natural orbital based explicitly correlated ccsd(f12*) using laplace transformation techniques," *J. Chem. Phys.* **145**, 234107 (2016).
 - ²⁶ Sebastian Dohm, Markus Bursch, Andreas Hansen, and Stefan Grimme, "Semiautomated transition state localization for organometallic complexes with semiempirical quantum chemical methods," *J. Chem. Theory Comput.* **16**, 2002–2012 (2020).
 - ²⁷ Florian Weigend and Reinhart Ahlrichs, "Balanced basis sets of split valence, triple zeta valence and quadruple zeta

- valence quality for h to rn: Design and assessment of accuracy,” *Phys. Chem. Chem. Phys.* **7**, 3297–3305 (2005).
- ²⁸ Florian Weigend, “Accurate coulomb-fitting basis sets for h to rn,” *Phys. Chem. Chem. Phys.* **8**, 1057–1065 (2006).
- ²⁹ Michael Dolg and Xiaoyan Cao, “Relativistic pseudopotentials: Their development and scope of applications,” *Chem. Rev.* **112**, 403–480 (2012).
- ³⁰ Thom H. Dunning, “Gaussian basis sets for use in correlated molecular calculations. i. the atoms boron through neon and hydrogen,” *J. Chem. Phys.* **90**, 1007–1023 (1989).
- ³¹ Florian Weigend, Andreas Köhn, and Christof Hättig, “Efficient use of the correlation consistent basis sets in resolution of the identity mp2 calculations,” *J. Chem. Phys.* **116**, 3175–3183 (2002).
- ³² Marco Häser and Reinhart Ahlrichs, “Improvements on the direct scf method,” *J. Comput. Chem.*
- ³³ David P. Tew, “Principal domains in local correlation theory,” *J. Chem. Theory Comput.* **15**, 6597–6606 (2019).
- ³⁴ Gerald Knizia, “Intrinsic atomic orbitals: An unbiased bridge between quantum theory and chemical concepts,” *J. Chem. Theory Comput.* **9**, 4834–4843 (2013).
- ³⁵ Oliver Masur, Denis Usvyat, and Martin Schütz, “Efficient and accurate treatment of weak pairs in local CCSD(T) calculations,” *J. Chem. Phys.* **139**, 164116 (2013).
- ³⁶ Martin Schütz, Oliver Masur, and Denis Usvyat, “Efficient and accurate treatment of weak pairs in local CCSD(T) calculations. II. Beyond the ring approximation,” *J. Chem. Phys.* **140**, 244107 (2014).
- ³⁷ Marco Häser and Jan Almlöf, “Laplace transform techniques in møller–plesset perturbation theory,” *J. Chem. Phys.* **96**, 489–494 (1992).
- ³⁸ Yang Guo, Christoph Riplinger, Ute Becker, Dimitrios G. Liakos, Yury Minenkov, Luigi Cavallo, and Frank Neese, “Communication: An improved linear scaling perturbative triples correction for the domain based local pair-natural orbital based singles and doubles coupled cluster method [DLPNO-CCSD(T)],” *J. Chem. Phys.* **148**, 011101 (2018).
- ³⁹ Qianli Ma and Hans-Joachim Werner, “Scalable electron correlation methods. 5. parallel perturbative triples correction for explicitly correlated local coupled cluster with pair natural orbitals,” *J. Chem. Theory Comput.* **14**, 198–215 (2018).
- ⁴⁰ Péter R. Nagy, Gyula Samu, and Mihály Kállay, “Optimization of the linear-scaling local natural orbital ccSD(t) method: Improved algorithm and benchmark applications,” *Journal of Chemical Theory and Computation* **14**, 4193–4215 (2018).
- ⁴¹ David P. Tew, “Explicitly correlated coupled-cluster theory with Brueckner orbitals,” *J. Chem. Phys.* **145**, 074103 (2016).
- ⁴² Emmanuel Giner, David P. Tew, Yann Garniron, and Ali Alavi, “Interplay between electronic correlation and metal–ligand delocalization in the spectroscopy of transition metal compounds: Case study on a series of planar cu²⁺ complexes,” *J. Chem. Theory Comput.* **14**, 6240–6252 (2018).
- ⁴³ Giovanni Li Manni, Daniel Kats, David P. Tew, and Ali Alavi, “Role of valence and semicore electron correlation on spin gaps in fe(ii)-porphyrins,” *J. Chem. Theory Comput.* **15**, 1492–1497 (2019).
- ⁴⁴ David P. Tew, Benjamin Helmich, and Christof Hättig, “Local explicitly correlated second-order møller–plesset perturbation theory with pair natural orbitals,” *J. Chem. Phys.* **135**, 074107 (2011).
- ⁴⁵ David P. Tew, “Chapter four - principal domains in f12 explicitly correlated theory,” in *New Electron Correlation Methods and their Applications, and Use of Advances in Quantum Chemistry*, Vol. 83, edited by Monika Musial and Philip E. Hoggan (Academic Press, 2021) pp. 83–106.
- ⁴⁶ Qianli Ma, Max Schwilk, Christoph Köppl, and Hans-Joachim Werner, “Scalable electron correlation methods. 4. parallel explicitly correlated local coupled cluster with pair natural orbitals (pno-lccsd-f12),” *J. Chem. Theory Comput.* **13**, 4871–4896 (2017).
- ⁴⁷ Fabijan Pavošević, Chong Peng, Peter Pinski, Christoph Riplinger, Frank Neese, and Edward F. Valeev, “SparseMaps—A systematic infrastructure for reduced scaling electronic structure methods. V. Linear scaling explicitly correlated coupled-cluster method with pair natural orbitals,” *J. Chem. Phys.* **146**, 174108 (2017).